COX6A2 deficiency leads to cardiac remodeling in human pluripotent stem cell-derived cardiomyocytes

Mengqi Jiang (jiangmengqi2016@163.com)
Peking University School of Basic Medical Sciences https://orcid.org/0000-0001-7328-7442

Yuanxiu Song
Peking University Third Hospital

Xi Chen
Peking University Third Hospital

Min Zhu
National Center for Cardiovascular Diseases China: Chinese Academy of Medical Sciences & Peking Union Medical College Fuwai Hospital

Wenjing Lu
National Center for Cardiovascular Diseases China: Chinese Academy of Medical Sciences & Peking Union Medical College Fuwai Hospital

Mingyu Wei
Peking University Third Hospital

Feng Lan
National Center for Cardiovascular Diseases China: Chinese Academy of Medical Sciences & Peking Union Medical College Fuwai Hospital

Ming Cui
Peking University Third Hospital

Yun Bai
Peking University School of Basic Medical Sciences

Research Article

Keywords: Human cardiomyocyte, Cardiac remodeling, COX6A2, hiPSCs, CRISPR/Cas9, Oxidative stress, Drug discovery

Posted Date: February 17th, 2023

DOI: https://doi.org/10.21203/rs.3.rs-2165236/v1

Version of Record: A version of this preprint was published at Stem Cell Research & Therapy on December 10th, 2023. See the published version at https://doi.org/10.1186/s13287-023-03596-x.

Abstract

Background: Cardiac remodeling is the initiating factor in the development of heart failure(HF), which can occur in various cardiomyopathies. cytochrome c oxidase subunit 6A2(COX6A2) is one of the components of cytochrome c oxidase, which drives oxidative phosphorylation. The pathogenesis of myocardial remodeling caused by COX6A2 deficiency in humans remains unclear due to the lack of a suitable research model. In this study, we established a COX6A2-deficient human cardiac myocyte(CM) model mimicking "human COX6A2 homozygous mutation" to explore the potential effects of COX6A2 dysfunction and its mechanism of action.

Methods: Human COX6A2 homozygous knockout cardiomyocytes model was established by combining CRISPR/Cas9 gene editing technology and hiPSCs directed differentiation technology. Cell model phenotypic assays were then performed to characterize the pathological features of COX6A2-deficient cardiomyocytes.

Results: COX6A2 gene knockout did not affect the pluripotency and differentiation efficiency of hiPSCs. Myocardial cells with COX6A2 gene knockout showed abnormal energy metabolism, increased oxidative stress level, abnormal calcium transport and decreased contractility. In addition, L-carnitine and trimetazidine significantly improved energy metabolism in COX6A2 deficient human myocardial model.

Conclusions: We have established a COX6A2-deficient human cardiomyocyte model that exhibits abnormal energy metabolism, elevated oxidative stress levels, abnormal calcium transport, and reduced contractility. This model is an important tool to help understand the mechanism of action of energy metabolism disorders leading to myocardial remodeling, elucidate the gene-phenotype relationship of COX6A2 deficiency, and facilitate drug screening.

Introduction

Cardiac remodeling refers to the pathological state of abnormal changes in cardiac structure, metabolism, and function caused by myocardial damage and/or increased load under the stimulation of various pathogenic factors, which is the initial factor of heart failure. At the molecular level, cardiac remodeling can be specifically manifested as cardiac chamber enlargement, apoptosis, excessive deposition or increased degradation of myocardial extracellular matrix, and fibrosis replacement, but the specific mechanism is not clear[1]. Although there are differences in the mechanisms of cardiac remodeling caused by different etiologies, the disorder of energy metabolism of cardiomyocytes is the final common pathway of cardiac remodeling[2]. Mitochondria are the main site of myocardial energy production and metabolism, accounting for 30% of the total volume of myocardial cells[3], and the energy produced can account for 90% of the total energy[4, 5]. The heart is the largest energy consuming organ in the human body and is the tissue with high energy demand. Mitochondria, as the main organelle for energy production, can account for 30% of the total volume of cardiomyocytes[6]. Therefore, maintaining

the integrity and function of mitochondria is very important for maintaining the normal structure and physiological function of myocardium.

Respiratory chain complex IV (cytochrome C oxidase, COX) is the terminal enzyme complex of the mitochondrial electron transport chain, which catalyzes the transfer of electrons from reduced cytochrome c to molecular oxygen and the transfer of protons to the inner mitochondrial membrane. The establishment of this electrochemical gradient across the membrane provides the driving force for ATP synthesis[7]. The COX6A protein is one of the 13 subunits of complex IV of the respiratory chain. Its exact role in this complex is unknown; Possible functions are assembly of the complex as well as regulation of the catalytic nature of the core subunit. Mammalian COX6A is represented by two distinct isoforms, Cox6a-L (COX6A1, hepatic type) and COX6A-H (COX6A2, cardiac type). The COX6A1 subunit is widely expressed, whereas COX6A2 expression is restricted to striated muscle[8, 9], but recent studies have found that COX6A2 is also found in nerve cells. So far, functional studies of COX6A2 are scarce. Only mice with COX6A2 gene knockout have been found to have diastolic cardiac dysfunction when cardiac load is increased[10], have a certain protective effect on insulin resistance[9], and COX6A2 can protect neurons from oxidative stress[11]. In terms of case reports, it has been reported that two patients with COX6A2 mutation presented with limb muscle weakness, hypotonia, and facial muscle weakness, and one of them had cardiomyopathy[12]. This suggests that COX6A2 indeed plays an important role in cardiomyocytes, and the aim of our study is to investigate the role of COX6A2 in maintaining the normal function of cardiomyocytes.

Methods

hiPSC culture and cardiac differentiation

The human induced pluripotent stem cells-U2 line(hiPSCs-U2, purchased from Cellapy, China) were cultured in six-well plates(Corning, USA) coated with Matrigel(Corning, USA) and cell medium was changed every day. When the cell confluence reaches 80%-90%, it is replaced with myocardial differentiation medium(Cellapy, China)[13]. On the 10th day of differentiation, cells that could beat autonomously appeared.

Genome Editing

COX6A2 single-stranded guide RNA (sgRNA)(GTGGCCTCCTTTGGCAGCGC)was designed on an online tool (https://design.synthego.com). We introduced the epiCRISPR vector with sgRNA into hiPSC by electroporation using the 4D nuclear receptor system (Lonza, Germany) and CA137 program. The treated cells were reseeded on six-well plates, and drug screening (puromycin) was initiated when the confluence of cells reached 40% to obtain homozygous transfection strains.

Immunofluorescent Staining

Cells were seeded on Matrigel-coated 20 mm coverslips and fixed with 4% PFA for 15min. Cells were membrane broken with 0.2% Triton X-100(Sigma, USA) and blocked with 3% BSA (Sigma, USA) for 30min. The primary antibody was incubated at 4°C overnight, and the secondary antibody (Invitrogen, USA) was incubated at 37°C for 1h in the dark. The cells were washed with PBS and fixed in fluorescent blocking tablets containing DAPI(4, 6-diamino-2-phenylindole). Images were taken under a confocal microscope (Leica DMI 4000B, Germany). Antibodies and their appropriate dilutions are provided in the additional file Table S1.

Western Blot

Western blot
Cells were digested and centrifuged, and then lysed using a protein extraction reagent (Thermo Fisher, USA) supplemented with a mixture of phosphatase and protease inhibitors(Thermo Fisher, USA). The entire cleavage process was carried out on ice and the samples were shaken every 10 min with an oscillator, then centrifuged(12,000 rpm, 15 min) and the supernatant was collected as the protein sample. Protein concentration was determined by BCA method. By gel electrophoresis, equal amounts of protein are arranged on a gel in order of protein size and then transferred to a polyvinylidene fluoride(PVDF) membrane. The membranes were blocked with 5% skim milk powder for 1h at 37°C and then incubated with the primary and secondary antibodies listed in the additional file Table S2.

Flow Cytometry

The detected cardiomyocytes were treated with CardioEasy Human Cardiomyocyte Digestive Fluid (Cellapy, China) to form a single cell suspension. After washing with PBS, cells were fixed (except for viable cell assays), then stained with different antibodies, re-filtered through a 300-mesh filter, and analyzed immediately with FACS (Beckman, USA). The number of cells tested in one group was not less than 1 million. The results were analyzed by Flow Jo program.

Rna Extraction And Quantitative Real-time Pcr

Total RNA from the cells to be tested was extracted by the TRIZOL Reagent (Invitrogen, USA) and then reverse transcribed into cDNA using the PrimeScrip Reverse Transcription system (Takara, Japan). Quantitative RT-PCR involved use of SYBR Green II (Takara, Japan) in the iQ5 system (Bio Rad, Hercules, CA). A comparative CT method was used to analyze the relative changes in gene expression. The results were expressed as relative to the data of β-actin transcripts (internal control). Primer sequences are listed in Additional file Table S2.

Transmission Electron Microscopy

The detected cardiomyocytes were treated with CardioEasy Human Cardiomyocyte Digestive Fluid (Cellapy, China). Then the cell suspension was centrifuged and fixed with 0.10% GA + 4% PFA. After dehydration, the sample was prepared and placed under transmission electron microscope (Thermo, USA) for image acquisition.

Seahorse

The cells to be tested were inoculated onto the cell culture plate, and the Seahorse XFe24 Flux Assay Kit was used, and then the Agilent Seahorse XFe24 system was used to detect the respiratory and reserve functions of the cells.

Ca Imaging

The cardiomyocytes to be tested were seeded in confocal, incubated with Fluo-4 (Beyotime, China), and the spontaneous calcium transient signals of cardiomyocytes were collected by confocal microscopy (Leica, USA) at high frame rate. The results were analyzed by Image J and IGOR Pro.

Detection Of Myocardial Contractility

The cells to be tested were cultured in six-well plates(Corning, USA) coated with Matrigel(Corning, USA). The video was shot by Leica DMI 4000B. Videos of cardiomyocyte beats were taken for 3–5 s, saved in the original .czi format, and then converted to an uncompressed .avi format (70 frames per second [fps]). A special plugin for video analysis(MUSCLEMOTION) is installed in Image J to analyze the results[14].

Detection Of Atp Content In Cells

200 μl lysate was added to each well of the 6-well plate, and the supernatant was collected after cell lysis. Then, the cells were examined using an ATP detection kit (Beyotime, China) and the relative light unit (RLU) values were measured with a luminometer or liquid scintillation meter to detect the ATP content in the cells. The concentration of ATP in the sample was calculated from standard curves and cell numbers.

Data Analysis And Statistics

Results are expressed as Mean ± SD. Statistical analysis was performed with GraphPad Prism 8.0.1 for Windows. Two-sided unpaired Student’s t test was used to compare

2 groups with normal distribution. One-way ANOVA was used to compare 3 or more groups. All tests for normality and homogeneity of variance were passed before t-test and one-way analysis of variance. P

values of less than 0.05 were used to denote statistical significance. *P < 0.05, **P < 0.01, ***P < 0.001; ns, not significant.

Results

Establishment of the COX6A2-deficient hiPSC model

We established a COX6A2-deficient hiPSC cell model using the CRISPR/Cas9 system. We designed sgRNA targeting the COX6A2 gene in cells and constructed plasmids containing sgRNA and Cas9 elements. The plasmid lapped with sgRNA was introduced into hiPSCs by electric transfer method, and the cells were screened by puromycin. The genotypes of the surviving clones were determined by Sanger sequencing. The results showed that homozygous COX6A2-knockout hiPSCs ($COX6A2^{-/-}$hiPSCs) was successfully obtained (Fig. 1A). $COX6A2^{-/-}$hiPSCs grew as clonogenic cell clusters as normal hiPSCs(Figure S1A). Immunofluorescence staining of stem cell markers OCT4 and SSEA4 was performed on the obtained cell lines, and the results indicated that COX6A2 knockout did not affect the expression of stemness markers of hiPSCs (Fig. 1B). Then we carried out karyotype detection on $COX6A2^{-/-}$hiPSCs, and found that $COX6A2^{-/-}$hiPSCs maintained normal karyotype (Fig. 1C). Furthermore, teratoma assays revealed that $COX6A2^{-/-}$hiPSCs preserved the ability to differentiate into three germ layers(Figure S1B). To verify the successful knockdown of COX6A2, we performed Western blot verification at the protein level, and the results showed that no significant COX6A2 protein expression was found in $COX6A2^{-/-}$hiPSCs (Fig. 1D, full-length blots are presented in Supplementary Fig. 2).

Cox6a2hipscs Showed Normal Myocardial Differentiation

In order to verify whether COX6A2 gene knockdown affects myocardial differentiation, we applied the original small molecule with clear chemical composition to induce hiPSCs directed cardiomyocyte differentiation technology to induce hiPSCs and $COX6A2^{-/-}$hiPSCs cells and observe their differentiation efficiency. This differentiation protocol can produce $TNNT2^{+}$ cardiomyocytes efficiently. We successfully induced hiPSCs and $COX6A2^{-/-}$hiPSCs to differentiate into cardiac myocytes hiPSC-CMs(WT) and $COX6A2^{-/-}$hiPSC-CMs(KO), respectively. Spontaneous and regular beating of reticular myocardium was observed from day 9 to 10 of differentiation.

To further explore the effect of COX6A2 knockdown on the differentiation of hiPSCs into hiPSC-CMs, the differentiation efficiency of cardiomyocytes in WT and KO groups was detected. TNNT2 is a protein specifically expressed in cardiomyocytes, which is usually used as a marker for cardiomyocyte detection[13]. TNNT2 and α-actinin are one of the most commonly used markers to detect the myofilaments and sarcomere structure of cardiomyocytes[15]. Immunofluorescence staining was used to detect TNNT2 and α-actinin in cardiomyocytes of the two groups, and the results showed that TNNT2 and α-actinin were normally expressed in cardiomyocytes of the two groups. The myofilaments and

sarcomere arrangement of KO cardiomyocytes were also very regular and clear, which preliminarily indicated that cardiomyocytes in both groups were normally differentiated (Fig. 2A). To further verify whether the differentiation efficiency of the two groups of cardiomyocytes was consistent, we used flow cytometry to detect TNNT2 labeling on the two types of cardiomyocytes cultured without purification on the 10th day of differentiation. The data showed that the expression ratio of TNNT2 in both WT and KO groups was about 80%. There was no statistical difference (Fig. 2B, C). These results indicated that the COX6A2 gene knockout human cardiomyocyte model was successfully established, and COX6A2 deletion did not affect the differentiation efficiency of cardiomyocytes.

Cox6a2hipsc-cms Showed Myocardial Remodeling Phenotype

Cardiac hypertrophy and myocardial remodeling occur in cardiomyocytes under pathological conditions, which are the initial factors leading to heart failure. To observe the effect of COX6A2 deletion on cardiomyocyte morphology, we first examined the cell size of COX6A2$^{-/-}$hiPSC-CMs. The two types of myocardium developed to 40 days were inoculated as cell crawling slices, and the cardiomyocyte cytoskeleton was stained with phalloidine, and the surface area of KO cardiomyocytes was significantly increased compared with WT cardiomyocytes by laser confocal microscopy (Fig. 3A). We further use of flow cytometry to test the two kinds of myocardial cell volume, the results show that compared with WT myocardial cell, KO myocardial cell "forward scattering Angle (FSC)" this metric peak obvious moves to the right (Fig. 3B, C), further verify the COX6A2 myocardial cell size significantly increased after missing, presents the hypertrophy myocardial morphology. Then we detected cardiac hypertrophy and heart failure-related markers Atrial natriuretic factor (ANP) and Brain natriuretic peptide (BNP) in KO cardiomyocytes[16]. Myocardial fibrosis occurs in the process of myocardial remodeling, affecting the function of cardiomyocytes, and type I collagen α1 chain (COL1A1) and type IV collagen α1 chain (COL4A1) play an important role in inhibiting the occurrence and development of myocardial fibrosis[17]. Myosin heavy chain α (MYH6) and myosin heavy chain β (MYH7) are two important subunits of myosin[18], which play a very important role in maintaining the normal myofilaments and sarcomere structure and function of cardiomyocytes. By Q-PCR, we found that compared with WT, the mRNA levels of ANP, BNP, COL1A1 and COL4A1 in cardiomyocytes after COX6A2 knockdown were significantly increased (Fig. 3D-G), suggesting that cardiomyocytes developed towards cardiac hypertrophy and fibrosis. At the same time, we also found that the expression levels of MYH6 and MYH7 in cardiomyocytes of WT and KO groups were not significantly different (Fig. 3H, I), which further suggested that COX6A2 deletion would not affect the structural stability of myofilaments and sarcomere of cardiomyocytes.

Mitochondrial Morphology And Function Were Affected In Cox6a2-deficient Cardiomyocytes

The normal form of mitochondria is very important to maintain their normal physiological function. Changes in mitochondrial function also affect mitochondrial morphology[19, 20]. To explore the effects of oxidative stress on mitochondrial function in cardiomyocytes caused by COX6A2 knockdown, mitochondrial functions were detected.

Firstly, we used transmission electron microscopy to visually observe the morphology of mitochondria in WT and KO groups of cardiomyocytes. After observation, we found that compared with WT cardiomyocytes, the size of mitochondria in KO cardiomyocytes was generally enlarged and the mitochondrial crista was relatively reduced (Fig. 4A). In this case, we also examined the mitochondrial DNA content of the two groups of cardiomyocytes to determine the comparison of the number of mitochondria between the two groups. Mitochondria encode NADH Dehydrogenase 1 and 2 (ND1, ND2) are proteins specifically Encoded by mitochondrial DNA, and can primarily reflect mitochondrial number[21]. We used Q-PCR technology to detect the contents of ND1 and ND2 in cardiomyocytes of the two groups, and it was found that the expressions of ND1 and ND2 in KO cardiomyocytes were significantly lower than those in WT group (Fig. 4B), indicating that COX6A2 knockout would lead to a decrease in the number of mitochondria in cardiomyocytes. To further clarify this result, we performed flow cytometry on both cardiomyocytes using the mitochondrial probe Mitotracker and also found that the mean fluorescence intensity of Mitotracker in KO cardiomyocytes was significantly lower than that in WT cardiomyocytes (Fig. 4C, F). These results indicated that COX6A2 knockdown would cause a decrease in the number of mitochondria in cardiomyocytes.

Reactive oxygen species (ROS) will be produced during cardiomyocyte aerobic metabolism. About 10% ROS is produced in the normal metabolic process of cells, and excessive intracellular ROS can cause damage to biological macromolecules such as lipids, proteins and nucleic acids in cells[22]. Oxidative stress injury caused by ROS and subsequent apoptosis of cardiomyocytes is one of the main causes of cardiomyopathy-related pathological phenotypes and even heart failure related phenotypes[23]. We used DCFH-DA to detect the ROS level of WT and KO cardiomyocytes, and found that the fluorescence intensity of KO cardiomyocytes was significantly reduced compared with WT cardiomyocytes (Fig. 4D, G), indicating that the ROS level of KO cardiomyocytes was significantly higher than that of WT cardiomyocytes.

The high oxygen environment of mitochondria means that more than 90% of intracellular O_2 is consumed in mitochondria. Most of the ROS produced by cardiomyocytes are generated in mitochondria. Therefore, in this experiment, we used MitoSOX Red, a new fluorescent dye specifically targeting mitochondrial superoxide in living cells, to detect the ROS levels in mitochondria of WT and KO cardiomyocytes. It was found that compared with WT cardiomyocytes, mitochondrial ROS in KO cardiomyocytes was significantly increased (Fig. 4E, H), indicating that the mitochondrial oxidative stress level of KO cardiomyocytes was significantly higher than that of WT cardiomyocytes.

Then, we detected the membrane potential level of WT and KO cardiomyocytes by immunofluorescence staining and JC-1 fluorescent probe. When the mitochondrial function was normal, the mitochondrial

membrane potential level was higher, and JC-1 fluorescent probe showed red fluorescence in general. When cells mitochondrial function is abnormal, the membrane potential is reduced, JC-1 fluorescent probe fluorescence from red to green fluorescent, fluorescent probe therefore JC-1 fluorescent from red to green fluorescence change can reflect the cell membrane potential drop, this transformation can be used as one of the direct detection of myocardial cell mitochondrial function index[24]. Laser confocal microscope observation showed that the proportion of red fluorescence in WT cardiomyocytes accounted for the majority, while the proportion of red fluorescence in KO cardiomyocytes significantly decreased and the proportion of green fluorescence significantly increased (Fig. 4I, J), suggesting that the mitochondrial membrane potential level of cardiomyocytes was significantly reduced after COX6A2 knockout. These results suggest that mitochondrial function is impaired, which is consistent with the phenomenon of cellular calcium overload. Cellular calcium overload can lead to the decrease of mitochondrial membrane potential.

Ca^{2+} in mitochondria is an important sensitive signal affecting mitochondrial function. Ca^{2+} overload in mitochondria of cardiomyocytes can cause the increase of mitochondrial ROS, thus affecting mitochondrial function.

Cox6a2-knockout Cardiomyocytes Showed Reduced Energy Metabolism

The contraction and relaxation of cardiomyocytes require sufficient energy support[25]. When the myocardial cell energy supply problems, the normal function of the heart muscle cells are badly affected, as a result, the myocardial cell energy metabolism disorder is considered a variety of development of the key factors for cardiovascular disease, especially in recent years, studies have shown that the energy metabolism of myocardial cell dysfunction in heart failure play a key role in the process of development[26].

ATP in normal cardiomyocytes is mainly produced by mitochondrial oxidative phosphorylation. To further measure the level of mitochondrial oxidative phosphorylation in WT and KO cardiomyocytes, we used the Seahorse XF assay to detect the level of mitochondrial oxidative phosphorylation in both groups of cardiomyocytes. The Oxygen Consumption Rate(OCR) and Extra Cellular Acidification Rate(ECAR) were used to reflect the mitochondrial function and glycolytic function, respectively. The curve of the final results (Fig. 5A) showed that basal respiration, maximal respiration and ATP production of KO cardiomyocytes were significantly lower than those of WT cardiomyocytes (Fig. 5B). At the same time, the extracellular acidification rate of KO cardiomyocytes was also significantly lower than that of WT cardiomyocytes, suggesting that the glycolytic capacity of KO cardiomyocytes was significantly reduced (Fig. 5C). These results indicate that both oxidative phosphorylation and glycolytic capacity of mitochondria are significantly reduced in COX6A2 knockout.

Combined with the previous experiments showing that COX6A2 knockout can lead to mitochondrial dysfunction in cardiomyocytes, we next studied the changes in energy metabolism of cardiomyocytes after COX6A2 knockout. In the case of sufficient oxygen supply in cardiomyocytes, most of the energy supply of cardiomyocytes comes from the fatty acid metabolism and glucose metabolism of cardiomyocytes to produce ATP for energy[27, 28]. Therefore, we first measured the expression of genes involved in fatty acid metabolism and glucose metabolism in WT and KO cardiomyocytes. First, we used Q-PCR to detect the relative expression levels of fatty acid metabolism-related genes in WT and KO cardiomyocytes. Twelve genes (ACSDG1, ACOT8, ACOT9, ACADVL, ACADM, HADHA, SLC27A6, FABP3, PRKAA2, PRKACA, PRKAG1, and PRKAG2) that were highly expressed in cardiomyocytes were selected for detection. The results suggested that the level of fatty acid metabolism was significantly reduced in COX6A2 knockout cardiomyocytes (Fig. 5D, E). We then examined the genes involved in glucose metabolism in the two groups of cardiomyocytes, Twelve glucose metabolism pathway-related genes (ALDOA, GPI, GYS1, IDH2, PGK1, PGM1, PGM3, GFPT1, TPI1, GAPDH, PDK4, SLC2A4) that were highly expressed in cardiomyocytes were also selected for detection. The overall trend of glucose metabolism in COX6A2 knockout cardiomyocytes was also found to be decreased (Fig. 5F, G). These results indicate that after COX6A2 knockout, KO cardiomyocytes show obvious metabolic disorders in both fatty acid metabolism and glucose metabolism pathways, and the energy supply of cardiomyocytes is insufficient, which is consistent with the pathological phenotype of myocardial remodeling.

Abnormal Calcium Transient In Hipsc-cms After Cox6a2 Knockout

In order to explore the molecular mechanism of dilated cardiomyopathy related pathological phenotypes in COX6A2 knockout cardiomyocytes, we used RNA seq technology to detect and analyze the changes of gene expression profiles in the two groups of cardiomyocytes. After analysis, a total of 1956 genes were significantly differentially expressed in KO cardiomyocytes compared with WT cardiomyocytes, of which 1111 genes were significantly up-regulated and 845 genes were significantly down-regulated (Fig. 6A). We performed KEGG (Kyoto Encyclopedia of Genes and Genomes) analysis on the two groups of WT and KO cardiomyocytes to understand the differences in the expression of pathways between the two groups of cardiomyocytes. The results showed (Fig. 6B) that cardiomyopathy-related pathways for Hypertrophic and Dilated cardiomyopathy were significantly enriched in KO cardiomyocytes compared with WT cardiomyocytes; Meanwhile, energy metabolism pathways were significantly enriched in KO cardiomyocytes, which was consistent with our previous experimental results. In addition, changes in calcium handling signaling pathways were also observed in KO cardiomyocytes, suggesting that calcium activity was also affected in COX6A2 KO cardiomyocytes.

Next, we examined the calcium transient in both groups of cardiomyocytes, in which we labeled Ca^{2+} using Fluo-4 AM probes. It was found that compared with WT cardiomyocytes, the Peak value of calcium transient in KO cardiomyocytes was significantly reduced and the Time to Peak time was significantly prolonged (Fig. 6C-F), indicating that there was an obvious barrier to calcium transient in KO cardiomyocytes.

The contractile function of cardiomyocytes is an important indicator to reflect the normal function of cardiomyocytes. Therefore, the contractile force level of cardiomyocytes in the two groups was detected at 40 days(Fig. 6G). The results showed that compared with WT cardiomyocytes, the contraction intensity of KO cardiomyocytes was significantly decreased (Fig. 6H). Meanwhile, the time to peak (Fig. 6I) and relaxation duration(Fig. 6J) were both significantly prolonged. In addition, we also found that the contraction frequency of KO cardiomyocytes was significantly decreased, suggesting that the heart rate of KO cardiomyocytes was reduced. These results suggest that loss of COX6A2 may cause myocardial dysfunction, which is one of the reasons for the myocardial remodeling phenotype in KO cardiomyocytes.

Improving Energy Metabolism Can Rescue The Myocardial Remodeling Phenotype Of Cox6a2-ko Hipsc-cms

Given the results of previous experiments showing that COX6A2 knockout leads to energy metabolism disorders in cardiomyocytes, and the levels of fatty acid and glucose metabolism in KO cardiomyocytes are significantly reduced, we selected Levo-carnitine (L-carnitine, LC) and Trimetazidine (TMZ). TMZ was used to improve the energy metabolism of KO cardiomyocytes. L-carnitine is an important cofactor in mitochondrial oxidation of fatty acids. It plays an important role in diseases related to metabolic disorders, especially mitochondria-related diseases. L-carnitine and its esters can improve mitochondrial dysfunction[29]. Trimetazidine decreased the level of pro-apoptotic protein BAX and increased the expression of Bcl-2. Trimetazidine increased the production of adenosine triphosphate (ATP) and the activity of superoxide dismutase (SOD) induced by myocardial infarction. It also reduced lipid peroxide (LPO), free fatty acid (FFA) and nitric oxide (NO) levels in a concentration-dependent manner[30]. L-carnitine mainly promotes fatty acid metabolism, and trimetazidine promotes the glycolytic process. After preliminary experiments, we explored the concentration gradient of the three therapeutic drugs, and finally determined the optimal concentration of LC 200 μmol/L and TMZ 50 μmol/L. The treatment time was LC and TMZ were added to the maintenance medium of human cardiomyocytes, and the solution was changed daily.

In order to explore the effects of the two drugs on the recovery of energy metabolism in KO cardiomyocytes, we first selected a simple and quick method to measure the ATP production of cardiomyocytes after various interventions. We used ATP detection kit to detect the ATP content of cardiomyocytes in each group after different drug intervention. The results showed that after the intervention of LC, TMZ, and LC + TMZ, the ATP content of KO cardiomyocytes was recovered to varying degrees, among which LC + TMZ had the best recovery effect(Fig. 7A). Combined with the characteristics of the two therapeutic drugs, we used Q-PCR to detect the treatment of LC on the fatty acid metabolism level of KO hiPSC-CMs and the recovery of TMZ on the glucose metabolism level of KO hiPSC-CMs. After testing, we can find that both drugs have better therapeutic improvement on the energy metabolism level of KO cardiomyocytes(Figure S3A,B). Similarly, ROS levels in cardiomyocytes were again examined after treatment with the three regimens, and the LC + TMZ group also showed the best ROS reduction(Fig. 7B). Then, we treated with LC and TMZ combination as the ultimate solution, the WT, KO and KO + LC + TMZ

three sets of myocardial cells in Seahorse experimental observation of living cells again levels between groups of myocardial energy metabolism, it was found that after joining drug intervention, KO myocardial cell energy metabolism level has obviously improved (Fig. 7C, D, E), It fully shows that the treatment of energy improvement related drugs is very effective. Finally, we also detected the calcium transient situation of cardiomyocytes after treatment, and after drug intervention, the level of calcium transport in cardiomyocytes was also restored to a certain extent(Fig. 7F, G), indicating that improving the energy metabolism level of COX6A2 deficient cardiomyocytes can restore the level of calcium activity in cardiomyocytes to a certain extent.

Discussion

Cardiac remodeling refers to the pathological state of abnormal changes in cardiac structure, metabolism and function caused by myocardial damage and/or increased load under the stimulation of various pathogenic factors, which is the initial factor of heart failure caused by various cardiovascular diseases[31]. However, the molecular mechanism of cardiac remodeling remains unclear. Therefore, it is of great significance to elucidate the molecular mechanism of cardiac remodeling, which can provide new ideas and basis for clinical prevention and treatment of heart failure. Although there are differences in the mechanisms of cardiac remodeling caused by different etiologies, the disorder of energy metabolism of cardiomyocytes is the final common pathway of cardiac remodeling[2].

Mitochondria are the most important place for myocardial energy production, so the maintenance of normal function and integrity of mitochondria is crucial for the maintenance of myocardial tissue structure and physiological function. However, it is difficult to perform high-throughput gene screening and pathway selection because primary human cardiomyocytes are difficult to sample and maintain stably in vitro. In addition, the commonly used mouse models differ greatly from the physiological characteristics of human cardiomyocytes, which cannot truly reflect the physiological state of the human body[32, 33]. Therefore, the study of mitochondrial function and cardiac remodeling is limited. At present, only a few proteins such as DRP1 and OPA1 are studied at the animal level[34, 35]. Therefore, new techniques and methods are needed to identify new members of mitochondrial function maintenance and explore their relationship with cardiac remodeling.

hPSCs are human pluripotent cells with the ability of self-renewal and self-replication. They can proliferate indefinitely in vitro and differentiate into cells of all germ layers, including cardiomyocytes. hiPSCs are an important type of hPSCs. Cardiomyocytes differentiated from hiPSCs by specific differentiation protocols in vitro contract spontaneously as in vivo cardiomyocytes, express sarcoplasmic reticulum proteins and ion channels, and have myocardial-specific action potential and calcium transient characteristics, which can mimic many phenotypes of human cardiomyocytes. It has become an important tool for human cardiovascular disease modeling and drug screening[36, 37]. In order to further study the mechanism of mitochondrial dysfunction and cardiac remodeling and break the species boundaries, hiPSC-CMs cell model was used. Our results fully demonstrated that the COX6A2-deficient

human cardiomyocytes model could well mimic the pathological phenotypes of myocardial remodeling. At the same time, because the COX6A2 homozygous knockout human cardiomyocytes model is a human cell model, it can avoid the species difference between animal models and human diseases, and its phenotypic characteristics and molecular mechanism are closer to the real human diseases, which is more convincing. The establishment of human COX6A2 homozygous knockout cardiomyocytes model helps to clarify the molecular mechanism of myocardial remodeling and provides a powerful tool for basic and clinical research.

Considering that COX6A2 functions as a functional protein in mitochondria, and mitochondria are the most important energy source of cells, we used a human COX6A2 homozygous knockout cardiac cell model to examine mitochondrial morphology and function as well as energy metabolism level before and after COX6A2 knockout. After observing the morphology of cardiomyocytes before and after COX6A2 knockout, we found that the mitochondrial morphology and function of cardiomyocytes were abnormal after COX6A2 knockout. However, after COX6A2 deletion, ROS accumulation and oxidative stress level are increased in cardiomyocytes. Mitochondria are the main sites of ROS production in cells, and the accumulation of ROS directly affects the function of mitochondria in cardiomyocytes. These results fully indicate that COX6A2 plays an important role in maintaining the normal structure and function of mitochondria.

Meanwhile, through high-throughput transcriptome sequencing analysis, we found enriched changes in intracellular calcium transport related pathways in cardiomyocytes. Combined with the results of Ca^{2+} transport experiments in WT and KO cardiomyocytes, we found that after COX6A2 deletion, the Ca^{2+} release and Ca^{2+} recovery time of KO cardiomyocytes were significantly prolonged, suggesting that the dysfunction of Ca^{2+} transport in KO cardiomyocytes leads to Ca^{2+} overload in cardiomyocytes.

When calcium overload occurs in cardiomyocytes, it can cause mitochondrial oxidative phosphorylation disorder, decrease of mitochondrial membrane potential, decrease of ATP production in cardiomyocytes, and increase of ROS level due to the activation of phospholipase and protease in cytoplasm, which can lead to and promote myocardial cell damage. COX6A2 knock out before at the same time, the contact can cause myocardial cell morphology and function obstacle, mitochondria increased mitochondrial ROS, reduced mitochondrial membrane potential and mitochondrial calcium overload, eventually there will be a "mitochondrial damage mitochondrial energy metabolism disorder-oxidative stress-mitochondrial dysfunction-abnormal myocardial cell calcium transport-mitochondrial damage" negative feedback loop, Aggravate the occurrence of myocardial cell-related pathological phenotypes.

According to its pathogenic mechanism, we have selected drugs with different targets to improve energy metabolism for intervention and treatment. Levo-carnitine and Trimetazidine were chosen to improve the energy metabolism of COX6A2-knockout cardiomyocytes. L-carnitine mainly promotes fatty acid metabolism, and trimetazidine promotes the glycolytic process. After treatment with L-carnitine and trimetazidine, the energy metabolism disorder of COX6A2 knockout cardiomyocytes was recovered, ATP production was increased, calcium transport was restored, and oxidative stress was reduced. In terms of

the degree of phenotypic recovery, the recovery effect of the combination of the two drugs was better, and it is reasonable to believe that there will be an additive effect of the combination of the two drugs, which is more conducive to restoring the level of energy metabolism of cardiomyocytes. Therefore, we infer that the combination of multiple drugs according to the patient's condition can better control the pathological development of myocardial remodeling and achieve the best therapeutic effect.

In summary, we have demonstrated that COX6A2 plays a critical role in the maintenance of energy metabolism and normal Ca^{2+} activity in cardiomyocytes. In this study, the molecular mechanism of myocardial remodeling induced by COX6A2 deletion was preliminarily elucidated.

Conclusions

In this study, we developed a COX6A2-deficient cardiac cell model using hiPSCs and CRISPR/Cas9 system in combination. To investigate the pathogenic mechanism of myocardial remodeling induced by COX6A2 deletion. This model can be used as an important tool to explore the mechanism of human heart-related diseases, determine the gene-phenotype correspondence, and facilitate the screening of new therapeutic drugs. The human cardiomyocytes model established in this study is a universal technology platform with highly customizable characteristics and broad prospects for clinical translation and application.

Abbreviations

hiPSC: human induced pluripotent stem cells; COX6A2: cytochrome c oxidase subunit 6A2; sgRNA: single-stranded guide RNA; GA: glutaric dialdehyde; PFA: Paraformaldehyde; hiPSC-CMs: human induced pluripotent stem cell derived cardiomyocytes; WT: Wild-type; PCR: Polymerase chain reaction; TNNT2: Troponin T; α-actinin: actinin alpha 1; KO: $COX6A2^{-/-}$hiPSC-CMs; LC: L-carnitine; TMZ: trimetazidine; KEGG: Kyoto Encyclopedia of Genes and Genomes.

Declarations

Ethical Approval and Consent to participate

Not applicable.

Availability of supporting data

All data generated or analyzed during this study are included in this published article.

Competing interests

The authors declare that they have no conflict of interest.

Funding

This project has been supported by the National Natural Science Foundation of China (Grant Nos. 81874166, 82070272) and the Natural Science Foundation of Beijing Municipality (Grant Nos. 7202225).

Author contributions

MQJ, YXS and WJL conceived the idea and designed the project. MQJ, YXS, MYW and XC performed most of the experiments and analyzed the data. MZ, MC, FL and YB provided technical assistance. MQJ wrote and revised the paper. All authors read and approved the final manuscript.

Acknowledgements

The authors thank the Cellapy Biological Technology Company (Beijing, CHN) for providing technical support for the hiPSC-CMs experiments.

Authors' information

1 Department of Cell Biology, School of Basic Medical Sciences, Peking University Health Science Center, Beijing, 100191, China.

2 Department of Cardiology, Peking University Third Hospital, 49 Huayuan North Road, Haidian District, Beijing 100191, China.

3 Shenzhen Key Laboratory of Cardiovascular Disease, Fuwai Hospital Chinese Academy of Medical Sciences, Chinese Academy of Medical Sciences and Peking Union Medical College, Shenzhen 518057, China.

4 Department of Emergency Medicine, The First Affiliated Hospital, School of Medicine, Zhejiang University, Hangzhou, 310003 Zhejiang, People's Republic of China.

5 Key Laboratory for Diagnosis and Treatment of Aging and Physic-chemical Injury Diseases of Zhejiang Province, Hangzhou, 310003 Zhejiang, People's Republic of China.

6 State Key Laboratory of Cardiovascular Disease, Fuwai Hospital, National Center for Cardiovascular Diseases, Chinese Academy of Medical Sciences and Peking Union Medical College, Beijing 100037, China.

References

1. Wu Q Q, Xiao Y, Yuan Y, et al. Mechanisms contributing to cardiac remodelling[J]. Clin Sci (Lond), 2017,131(18):2319–2345.
2. Gibb A A, Hill B G. Metabolic Coordination of Physiological and Pathological Cardiac Remodeling[J]. Circ Res, 2018,123(1):107–128.

3. Rossini M, Filadi R. Sarcoplasmic Reticulum-Mitochondria Kissing in Cardiomyocytes: Ca(2+), ATP, and Undisclosed Secrets[J]. Front Cell Dev Biol, 2020,8:532.
4. Rosca M G, Tandler B, Hoppel C L. Mitochondria in cardiac hypertrophy and heart failure[J]. J Mol Cell Cardiol, 2013,55:31–41.
5. Zhou L Y, Liu J P, Wang K, et al. Mitochondrial function in cardiac hypertrophy[J]. Int J Cardiol, 2013,167(4):1118–1125.
6. Vasquez-Trincado C, Garcia-Carvajal I, Pennanen C, et al. Mitochondrial dynamics, mitophagy and cardiovascular disease[J]. J Physiol, 2016,594(3):509–525.
7. Jager S, Handschin C, St-Pierre J, et al. AMP-activated protein kinase (AMPK) action in skeletal muscle via direct phosphorylation of PGC-1alpha[J]. Proc Natl Acad Sci U S A, 2007,104(29):12017–12022.
8. Kadenbach B, Barth J, Akgun R, et al. Regulation of mitochondrial energy generation in health and disease[J]. Biochim Biophys Acta, 1995,1271(1):103–109.
9. Quintens R, Singh S, Lemaire K, et al. Mice deficient in the respiratory chain gene Cox6a2 are protected against high-fat diet-induced obesity and insulin resistance[J]. PLoS One, 2013,8(2):e56719.
10. Radford N B, Wan B, Richman A, et al. Cardiac dysfunction in mice lacking cytochrome-c oxidase subunit VIaH[J]. Am J Physiol Heart Circ Physiol, 2002,282(2):H726-H733.
11. Sanz-Morello B, Pfisterer U, Winther H N, et al. Complex IV subunit isoform COX6A2 protects fast-spiking interneurons from oxidative stress and supports their function[J]. EMBO J, 2020,39(18):e105759.
12. Inoue M, Uchino S, Iida A, et al. COX6A2 variants cause a muscle-specific cytochrome c oxidase deficiency[J]. Ann Neurol, 2019,86(2):193–202.
13. Burridge P W, Matsa E, Shukla P, et al. Chemically defined generation of human cardiomyocytes[J]. Nat Methods, 2014,11(8):855–860.
14. Grune T, Ott C, Haseli S, et al. The "MYOCYTER" - Convert cellular and cardiac contractions into numbers with ImageJ[J]. Sci Rep, 2019,9(1):15112.
15. Ni X, Xu K, Zhao Y, et al. Single-cell analysis reveals the purification and maturation effects of glucose starvation in hiPSC-CMs[J]. Biochem Biophys Res Commun, 2021,534:367–373.
16. Goetze J P, Bruneau B G, Ramos H R, et al. Cardiac natriuretic peptides[J]. Nat Rev Cardiol, 2020,17(11):698–717.
17. Frangogiannis N G. Cardiac fibrosis[J]. Cardiovasc Res, 2021,117(6):1450–1488.
18. Toepfer C N, Garfinkel A C, Venturini G, et al. Myosin Sequestration Regulates Sarcomere Function, Cardiomyocyte Energetics, and Metabolism, Informing the Pathogenesis of Hypertrophic Cardiomyopathy[J]. Circulation, 2020,141(10):828–842.
19. Tilokani L, Nagashima S, Paupe V, et al. Mitochondrial dynamics: overview of molecular mechanisms[J]. Essays Biochem, 2018,62(3):341–360.

20. Yapa N, Lisnyak V, Reljic B, et al. Mitochondrial dynamics in health and disease[J]. FEBS Lett, 2021,595(8):1184–1204.
21. Quiros P M, Goyal A, Jha P, et al. Analysis of mtDNA/nDNA Ratio in Mice[J]. Curr Protoc Mouse Biol, 2017,7(1):47–54.
22. Singh A, Kukreti R, Saso L, et al. Oxidative Stress: A Key Modulator in Neurodegenerative Diseases[J]. Molecules, 2019,24(8).
23. Zhang S, Liu X, Bawa-Khalfe T, et al. Identification of the molecular basis of doxorubicin-induced cardiotoxicity[J]. Nat Med, 2012,18(11):1639–1642.
24. El-Hattab A W, Scaglia F. Mitochondrial Cardiomyopathies[J]. Front Cardiovasc Med, 2016,3:25.
25. Fink B D, Bai F, Yu L, et al. Regulation of ATP production: dependence on calcium concentration and respiratory state[J]. Am J Physiol Cell Physiol, 2017,313(2):C146-C153.
26. Doenst T, Nguyen T D, Abel E D. Cardiac metabolism in heart failure: implications beyond ATP production[J]. Circ Res, 2013,113(6):709–724.
27. Lopaschuk G D, Ussher J R, Folmes C D, et al. Myocardial fatty acid metabolism in health and disease[J]. Physiol Rev, 2010,90(1):207–258.
28. Bianchi V E. Impact of Nutrition on Cardiovascular Function[J]. Curr Probl Cardiol, 2020,45(1):100391.
29. Bin A S, Hussain M M, Farooq Y. Levo-carnitine reduces oxidative stress and improves contractile functions of fast muscles in type 2 diabetic rats[J]. Iran Biomed J, 2013,17(1):29–35.
30. Marzilli M, Vinereanu D, Lopaschuk G, et al. Trimetazidine in cardiovascular medicine[J]. Int J Cardiol, 2019,293:39–44.
31. Nakamura M, Sadoshima J. Mechanisms of physiological and pathological cardiac hypertrophy[J]. Nat Rev Cardiol, 2018,15(7):387–407.
32. Kloos W, Katus H A, Meder B. Genetic cardiomyopathies. Lessons learned from humans, mice, and zebrafish[J]. Herz, 2012,37(6):612–617.
33. Matsa E, Burridge P W, Wu J C. Human stem cells for modeling heart disease and for drug discovery[J]. Sci Transl Med, 2014,6(239):236p-239p.
34. Jin J Y, Wei X X, Zhi X L, et al. Drp1-dependent mitochondrial fission in cardiovascular disease[J]. Acta Pharmacol Sin, 2021,42(5):655–664.
35. Bean C, Audano M, Varanita T, et al. The mitochondrial protein Opa1 promotes adipocyte browning that is dependent on urea cycle metabolites[J]. Nat Metab, 2021,3(12):1633–1647.
36. Lan F, Lee A S, Liang P, et al. Abnormal calcium handling properties underlie familial hypertrophic cardiomyopathy pathology in patient-specific induced pluripotent stem cells[J]. Cell Stem Cell, 2013,12(1):101–113.
37. Caputo L, Granados A, Lenzi J, et al. Acute conversion of patient-derived Duchenne muscular dystrophy iPSC into myotubes reveals constitutive and inducible over-activation of TGFbeta-dependent pro-fibrotic signaling[J]. Skelet Muscle, 2020,10(1):13.

Figures

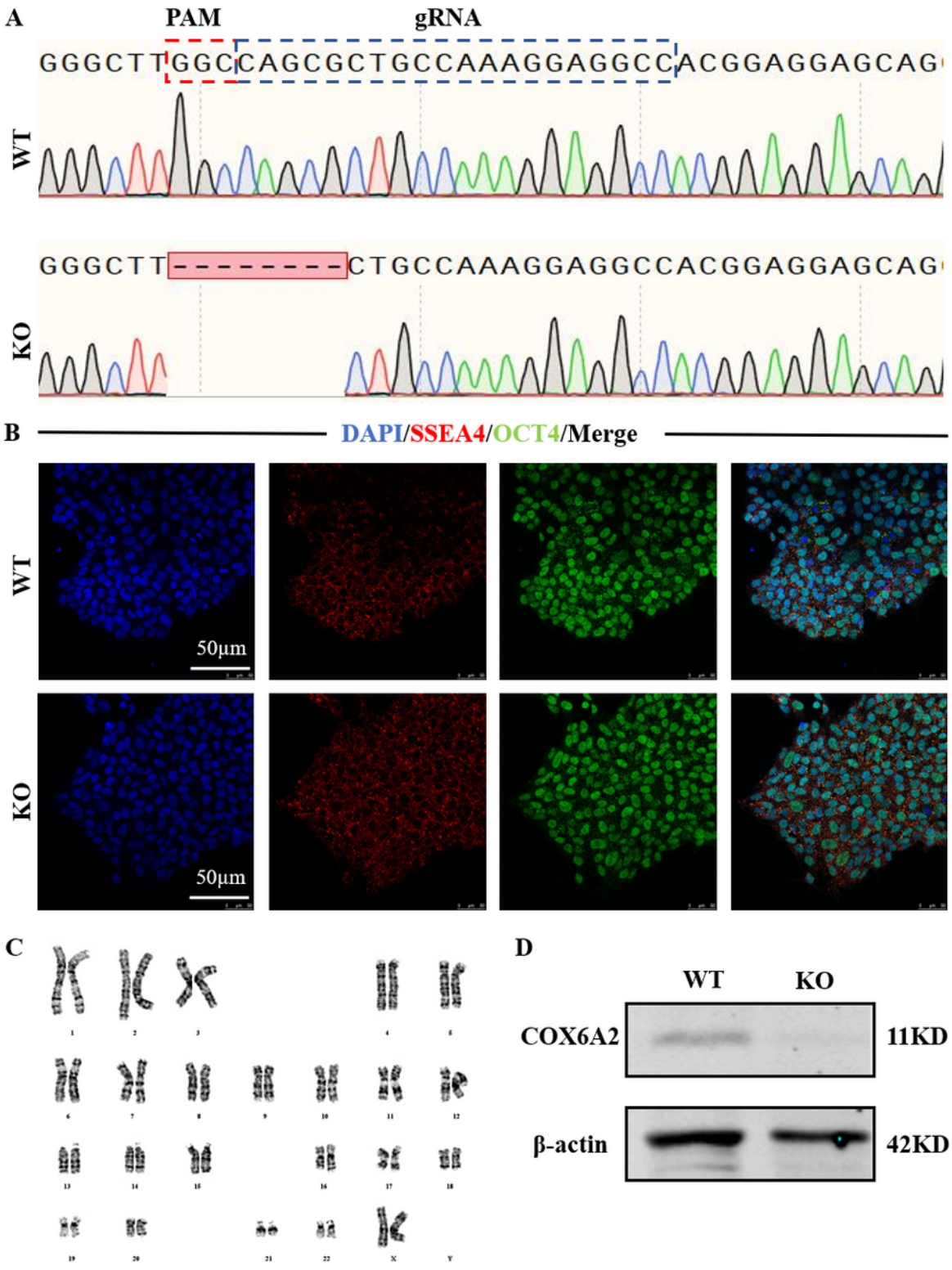

Figure 1

Establishment of COX6A2$^{-/-}$hiPSCs. (A) Diagram of the COX6A2 knockout pattern, showing the gene editing position and deleted base pair. (B) Immunofluorescence staining of COX6A2$^{-/-}$hiPSCs showed that

COX6A2$^{-/-}$hiPSCs expressed OCT4 and SSEA4 normally , scale bar=50 μm. C The karyotype analysis of KO-hiPSCs showed that KO-hiPSCs had normal female chromosomes. (D) COX6A2 protein could not be detected in KO-hiPSCs.

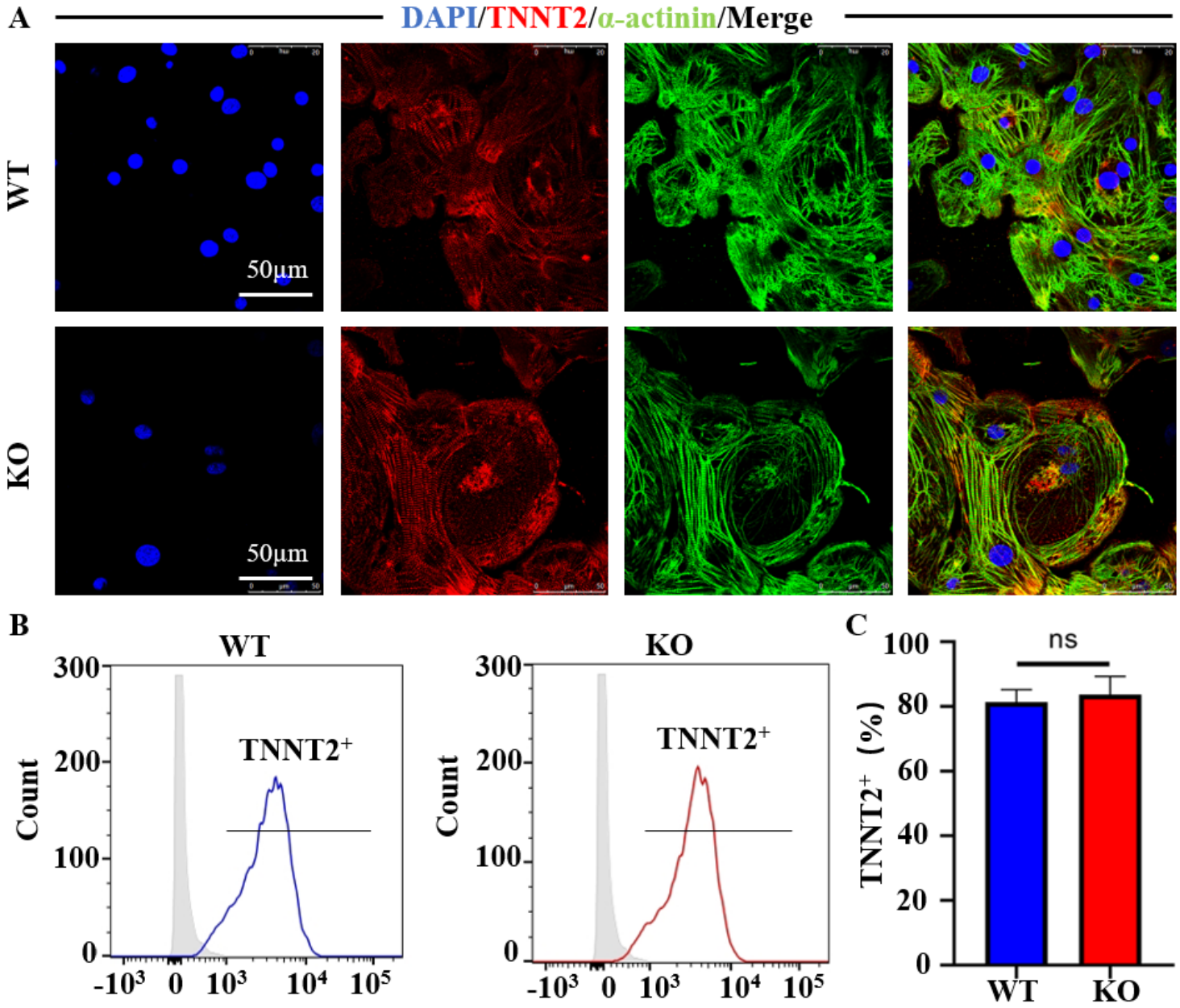

Figure 2

COX6A2 knockout did not affect the myocardial differentiation of hiPSCs. (A) COX6A2$^{-/-}$hiPSC-CMs normally expressed TNNT2 and α-actinin, and the myofilament were arranged neatly. (B) Flow cytometry was used to detect the positive rate of TNNT2 in unpurified WT and KO cardiomyocytes on day 10, and the results showed that the differentiation efficiency of cardiomyocytes in both groups was about 80%. (C) Quantitative statistical plot of the differentiation efficiency of WT and KO cardiomyocytes, and the statistical results showed that there was no statistically significant difference in the differentiation

efficiency of cardiomyocytes between the two groups. The results are presented as Mean ± SD of 3 independent experiments. ns, not significant.

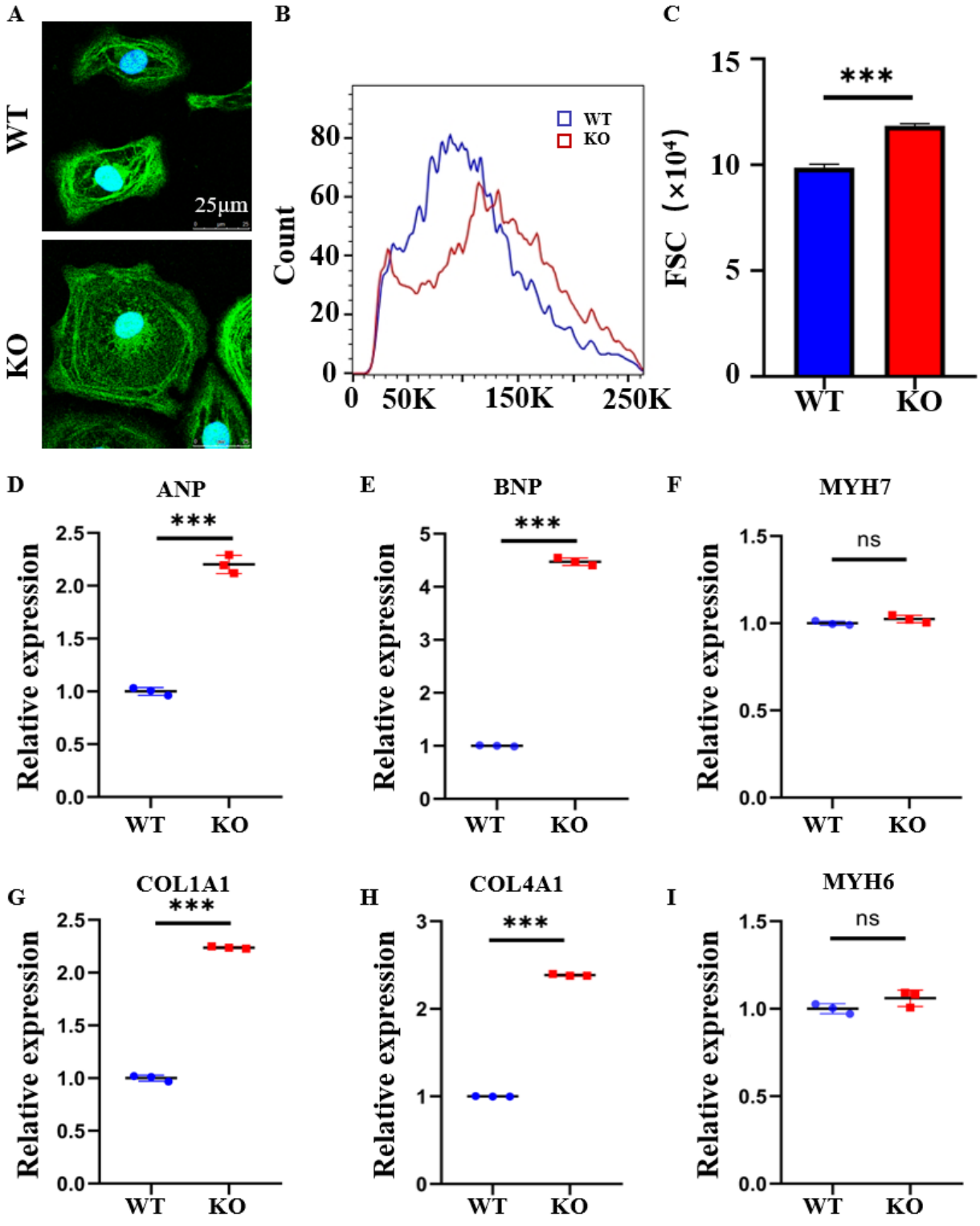

Figure 3

KO hiPSC-CMs showed increased cell size and a myocardial remodeling phenotype. (A) The size of WT and KO hiPSC-CMs was detected by phalloidin staining, and the volume of KO cardiomyocytes was

significantly larger, scale bar=25 μm). (B) The FSC measured by flow cytometry was used to compare the size of WT and KO hiPSC-CMs, and the results showed that the peak value of KO hiPSC-CMs was significantly shifted to the right and the cell volume was increased. (C) Quantitative statistical plots of FSC values in WT and KO hiPSC-CMs showed that the volume of KO cardiomyocytes was 1.3-fold larger than that of WT hiPSC-CMs. (D)(E)(F)(G)(H)(I) The expression levels of ANP, BNP, COL1A1, COL4A1, MYH7 and MUH6 in WT and KO hiPSC-CMs were detected by Q-PCR, suggesting that KO cardiomyocytes showed a myocardial remodeling phenotype. The results are presented as Mean ± SD of 3 independent experiments. ns, not significant; ***p 0.001.

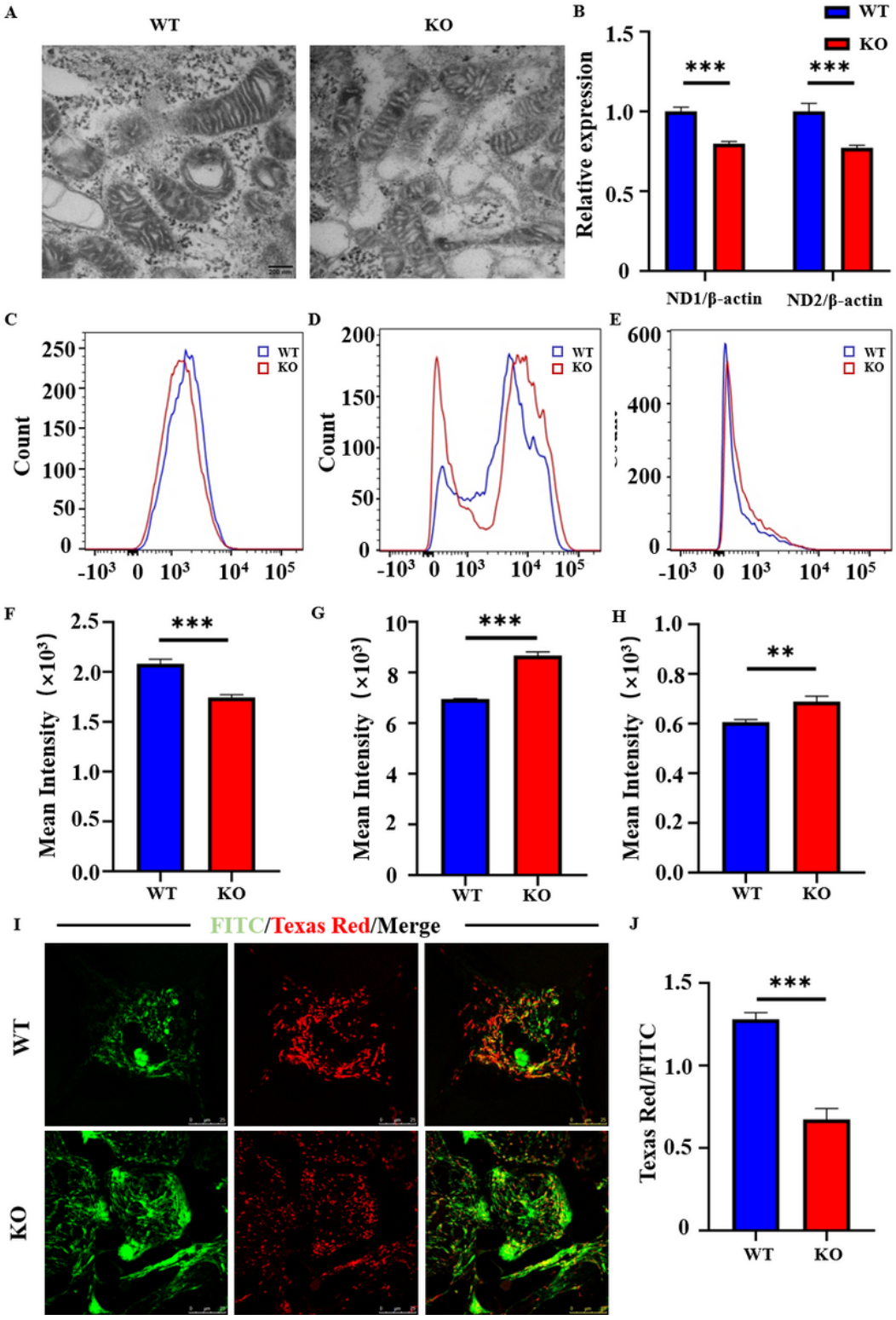

Figure 4

KO hiPSC-CMs showed abnormal mitochondrial function and elevated oxidative stress levels. (A) The mitochondrial morphology of WT and KO hiPSC-CMs was detected by transmission electron microscopy, suggesting that the mitochondrial morphology of KO hiPSC-CMs was abnormal. (B) The expression levels of ND1 and ND2 in WT and KO hiPSC-CMs were detected by Q-PCR, and the expression of ND1 and ND2 was down-regulated in KO cardiomyocytes, suggesting that mitochondrial DNA was reduced in KO

hiPSC-CMs. (C) Flow cytometry (Mitotracker labeling) showed the average fluorescence intensity distribution of mitochondria in WT and KO hiPSC-CMs. (D) The mean fluorescence intensity distribution of mitochondrial ROS in WT and KO hiPSC-CMs was detected by flow cytometry. (E) Flow cytometry (MitoSOX Red labeling) showed the mean fluorescence intensity distribution of mitochondrial ROS in WT and KO hiPSC-CMs. (F)(G)(H) Statistical plots for Mitotracker, ROS and MitoSOX values quantification of WT and KO hiPSC-CMs. (I) The mitochondrial membrane potential levels of WT and KO hiPSC-CMs were detected by immunofluorescence staining (JC-1 labeling), and the results showed that the mitochondrial membrane potential of KO hiPSC-CMs was decreased. (J) Statistical plots for JC-1 values quantification of WT and KO hiPSC-CMs. The results are presented as Mean ± SD of 3 independent experiments. ns, not significant; **p 0.01, ***p 0.001.

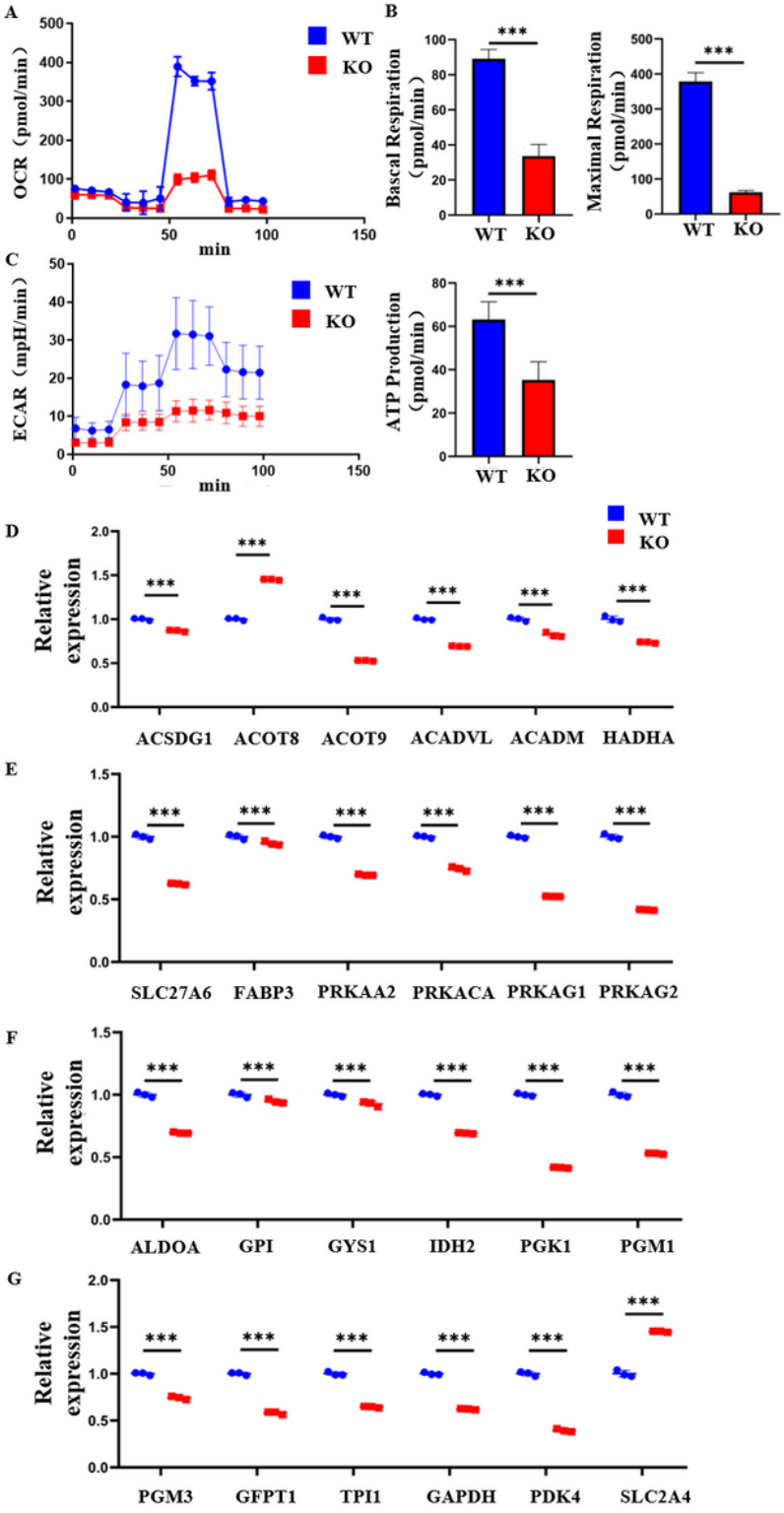

Figure 5

The energy metabolism level of KO hiPSC-CMs was affected. (A) The OCR curves of WT and KO hiPSC-CMs were detected by Seahorse experiments, suggesting that the aerobic respiration level of KO hiPSC-CMs was reduced. (B) Quantitative statistical analysis of basal and maximal respiration levels in WT and KO hiPSC-CMs indicated that basal and maximal respiration levels were decreased in KO hiPSC-CMs. (C) The ECAR curves of WT and KO hiPSC-CMs were detected by Seahorse experiments, suggests that the

level of glycolysis is reduced in KO hiPSC-CMs. (D)(E) The expression levels of fatty acid metabolism-related genes in WT and KO hiPSC-CMs were detected by Q-PCR. (F)(G) The expression levels of genes related to glucose metabolism in WT and KO hiPSC-CMs were detected by Q-PCR. The results are presented as Mean ± SD of 3 independent experiments. ***p 0.001.

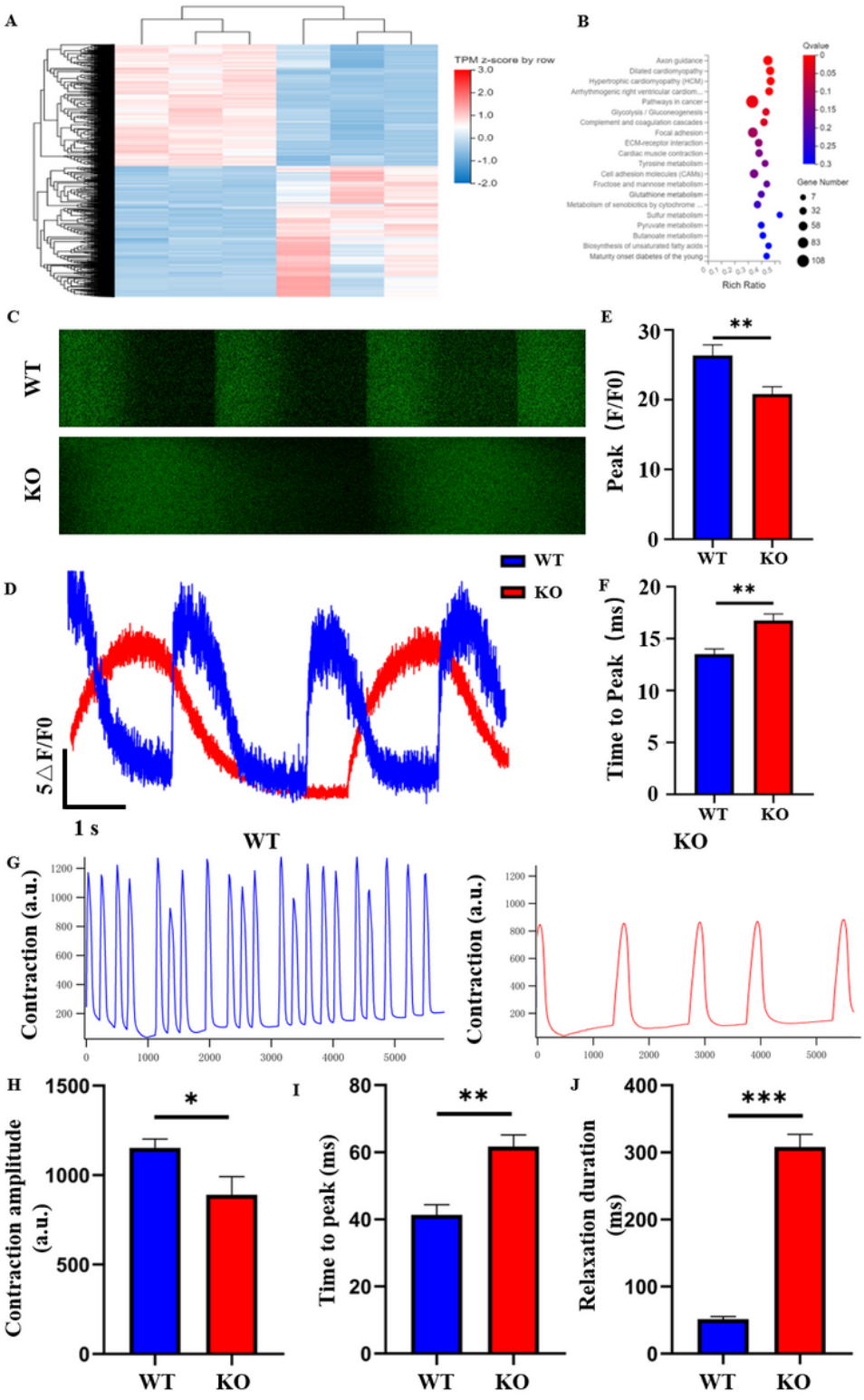

Figure 6

COX6A2 knockout affects calcium activity in cardiomyocytes. (A) RNA Seq was used to detect differentially expressed genes in WT and KO hiPSC-CMs. (B) KEGG analysis of pathway enrichment changes in KO hiPSC-CMs. (C) Ca^{2+} transient fluorescence patterns of WT and KO hiPSC-CMs were observed by confocal (Fluo-4 AM labeling). (D) Waveform plots of Ca2+ transients in WT and KO hiPSC-CMs. (E) Quantitative statistical plots of the Peak of Ca^{2+} transients in WT and KO hiPSC-CMs, which are decreased in KO hiPSC-CMs. (F) Quantitative statistical plots of the Time to Peak of Ca^{2+} transients in WT and KO hiPSC-CMs, which are increased in KO hiPSC-CMs. (G) Waveform plots of contractile force in WT and KO hiPSC-CMs, showing reduced frequency and intensity of contraction in KO hiPSC-CMs. (H) Quantitative statistical plot of contraction in WT and KO hiPSC-CMs, which showed reduced contractile intensity in KO hiPSC-CMs. (I) Quantitative statistical plot of time to peak in WT and KO hiPSC-CMs, time to peak in KO hiPSC-CMs was longer than that in WT hiPSC-CMs. (J) Quantitative statistical plots of relaxation time in WT and KO hiPSC-CMs showed that KO hiPSC-CMs had significantly longer relaxation time. The results are presented as Mean ± SD of 3 independent experiments. *P < 0.05, **P < 0.01, ***p 0.001.

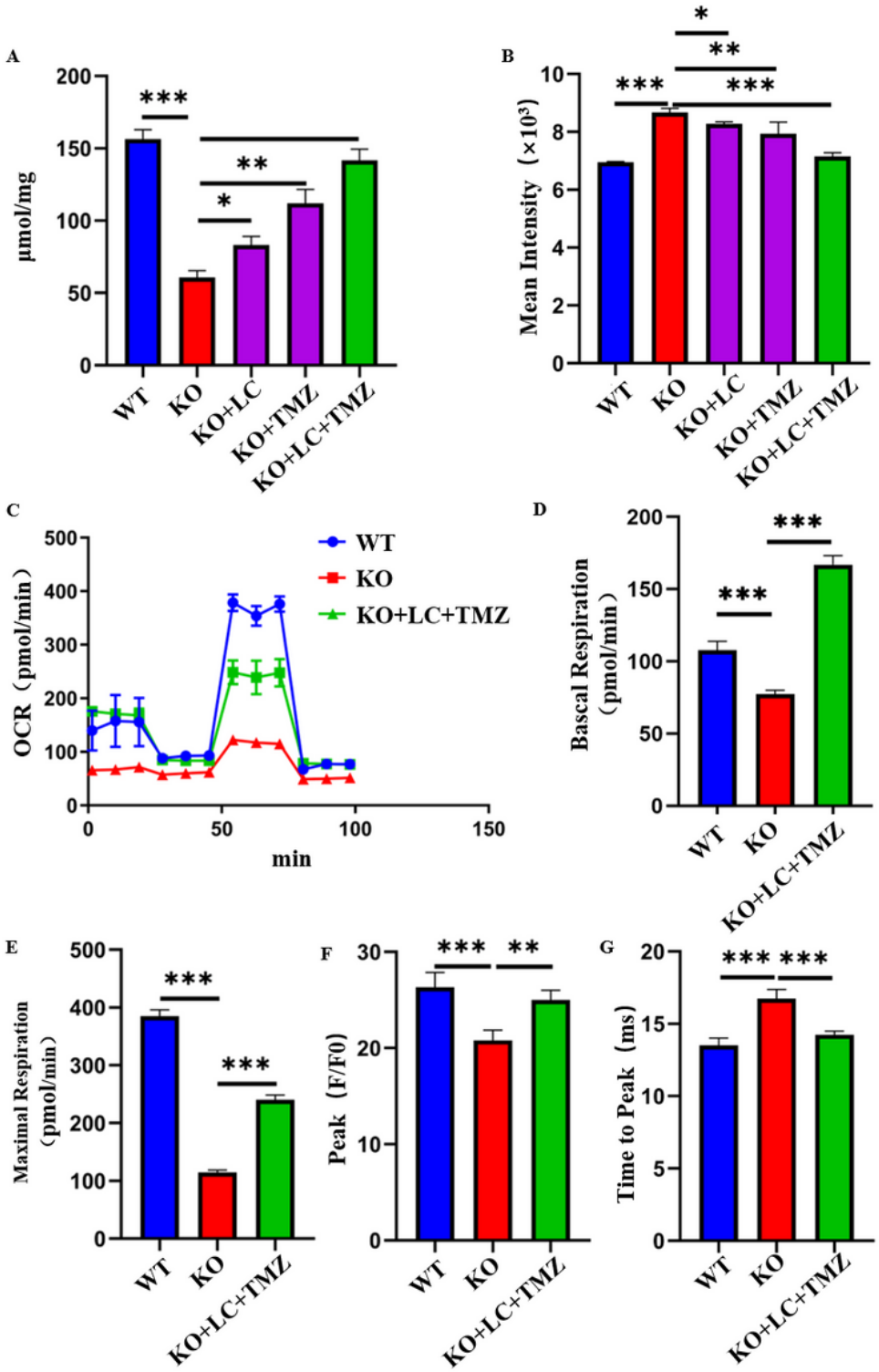

Figure 7

Application of energy-improving drugs can significantly correct the pathological phenotype of KO hiPSC-CMs. (A) The ATP content of WT, KO, KO+LC, KO+TMZ and KO+LC+TMZ groups was detected, and the results showed that the ATP level of KO hiPSC-CMs increased to varying degrees after different drug treatment. (B) ROS levels in WT, KO, KO+LC, KO+TMZ and KO+LC+TMZ groups were detected, and the results showed that ROS levels in KO hiPSC-CMs were reduced to varying degrees after different

treatments. (C) The OCR curves of WT, KO and KO+LC+TMZ hiPSC-CMs were detected by Seahorse experiments, the results showed that oxidative phosphorylation was restored in KO hiPSC-CMs after treatment. (D) The basal respiration level of KO hiPSC-CMs was restored after treatment. (E) The maximal respiration level of KO hiPSC-CMs was restored after treatment. (F) The peak level of calcium transient in KO hiPSC-CMs was somewhat restored after treatment. (G) The peak time of calcium transient in KO hiPSC-CMs was significantly decreased after treatment. The results are presented as Mean ± SD of 3 independent experiments. *P < 0.05, **P < 0.01, ***p 0.001.

Supplementary Files

This is a list of supplementary files associated with this preprint. Click to download.

- table.docx
- supplementarymaterial.docx